

Analysis of Pre-Emphasis Techniques for Channels with Higher-Order Transfer Function

B. Ševčík, L. Brančík, and M. Kubíček

Abstract— A transmitter pre-emphasis techniques to overcome high-slope losses of printed circuit board (PCB) with higher-order transfer function used in high-speed serial link design is presented. The pre-emphasis technique based on pulse-width modulation (PWM) using timing resolution instead of amplitude resolution to adjust the filter transfer function is analyzed and applied to channel with high-order transfer function. Leading-edge digital silicon manufacturing processes are pushing the maximum swing below 1.0 V and just PWM scheme is a good alternative for these cases. In addition only one coefficient can be used to set equalizer transfer function in depending on channel properties. Standard approaches to transmitter pre-emphasis and novel PWM pre-emphasis are compared in advanced PCB backplane model.

Keywords— Transmitter pre-emphasis, transfer function, pulse-width modulation, signal integrity, high-order.

I. INTRODUCTION

THE continuous development of high-speed serial communication systems leads to finding new solutions to create a reliable communication between devices that operate at frequencies above 1 GHz. Mathematical modeling of dynamic systems include a wide range of scientific areas, such as in [1]–[4]. In this frequency band it is necessary to accurately predict signal integrity (SI) problems that cause a significant reduction in system reliability. These problems in the design of high-speed serial devices and proposed solutions are discussed in this paper. Today, all the trends to higher switching speeds and the voltages provided on supply rails are going down. One of the biggest problems results from the commercial requirements is to reduce manufacturing costs. The cheaper components, packages, and substrates are still used in modern high-speed systems. In chip to chip communications, parallel data links require more pins, which increase the cost of packaging [5], [6]. Therefore, in high-speed data links, serial communications are replacing parallel communications rapidly. According to [7] packaging already represents 25% of the total system cost in some electronic products. There are many sources of impairments in the physical channel [8], [9] and just equalization method (often called pre-emphasis at the transmitter side) is the best solution

to overcome the significant channel losses. Pre-emphasis methods found in the literature are commonly based on Symbol-Spaced Finite Impulse Response (SSFIR) filtering [10], [11], [12]. In this paper, we describe the application of PWM pre-emphasis to the equalization of PCB differential transmission lines. It provides an alternative to FIR pre-emphasis with advantages in the light of developments in CMOS scaling. Our area of study is limited to electronic circuits for high speed serial links over PCB copper interconnects. To fully understand the factors that limit the link performance, we first make an introduction to find out how the communication channel between the two high-speed link chips degrades the signal. In the next section the transmission channel environment using a self-designed PCB evaluation backplane with higher-order transfer function is analyzed based on the advanced models developed in MathCAD [15]. The main part of the paper describes the analysis, implementation and tests both pre-emphasis techniques to increase the data rate of communication over copper channels.

II. TRANSMISSION CHANNEL

Prediction of accurate values for insertion loss (S_{21}) on printed circuit boards has become ever more critical to SI modeling as signal speeds required for next-generation networking equipment move into the 10+ GHz range. In high-speed data communication over PCB backplane, dielectric losses, conductor losses and effect of roughness cause inter-symbol interference (ISI), decreasing the eye opening and thus limiting achievable data rates.

A. Channel Design Specification

The PCB transmission channels based on FR4 dielectric are typically characterized by high slopes at frequencies above 1 GHz. The measured frequency response, including the simple circuit schematic of analyzed PCB backplane is shown in Fig.1. In most cases, the transfer function (S_{21}) is monotonically decreasing with increasing channel losses at higher frequencies. This situation corresponds approximately with theoretical channel CH2 (BW_{3dB}) analyzed together with more complicated channel transfer function in section III, see Fig. 10. Channel losses at the analyzed Nyquist frequency $f_N = 2.5$ GHz for maximal 5 Gbps data rate corresponds with 20 dB loss for both measured and theoretical channel.

This work was supported by the Czech Ministry of Education under the MSM 0021630503 Research Project MIKROSYN and Czech Science Foundation projects GAČR No. GD102/08/H027 and No. 102/09/1681.

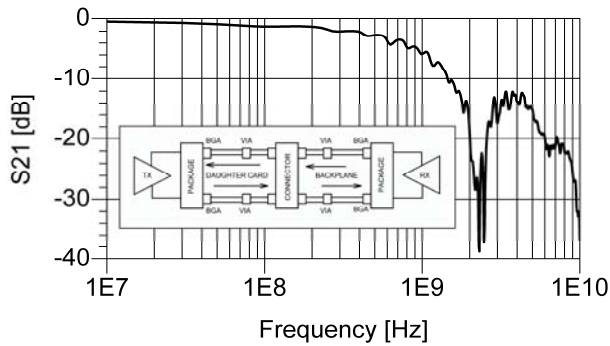


Fig. 1 Frequency response of analyzed transmission channel with two differential lines, vias, bga's and package models are included.

The analyzed backplane environment in Fig. 1 consists of two differential transmission line pair. In high-speed serial communication systems these structures are typically characterized with closely-spaced transmission lines where the edge-to-edge distances between adjacent lines are about 100 μm, with the widths of the signal traces also being equal 100 μm. Separation distance (SD) between pairs is chosen deliberately to 130 μm. The conductor widths (W) are 130 μm. The advanced model and analyzed backplane consist of two board traces as can be seen in Fig. 1. The first board trace is 10 cm long and the second board trace is 30 cm long. In [13] the PCIe2 analysis is shown and the significant impact of closely route groups of transmission lines on 3 dB transmission channel bandwidth (BW_{3dB}) is clearly demonstrated. The advanced numerical model has been developed in ADS2009 environment [14]. For channel losses modeling the Mathcad environment have been used [15].

The eye diagrams for 2 Gbps data rate and 4 Gbps data rate are shown in Fig. 2. The complete eye closure at 4 Gbps (2PAM signaling) is evidently. The losses of the analyzed channel are approximately 14 dB at the Nyquist frequency $f_N = 2$ GHz for 4 Gbps, see Fig. 1. The better response for 2 Gbps is shown in Fig. 4b. The losses of the analyzed channel are approximately 6 dB at the Nyquist frequency of 1 GHz for 2 Gbps, see Fig. 1. If we consider that the 3 dB channel loss have negligible effect on signal quality, additional 6-dB loss is sufficient to completely close the eye.

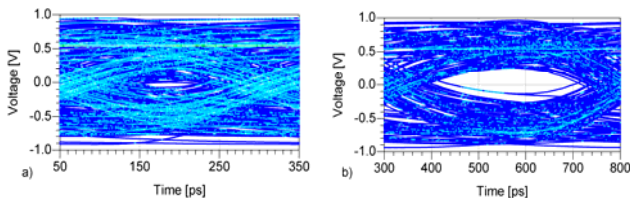


Fig. 2 Eye diagram analysis for data rates: a) 4 Gbps, b) 2 Gbps.

Note that the 6-dB rule is independent of voltage swing and frequency. What does depend on frequency is where the 6-dB loss point actually occurs. It is obvious that the communication system is reliable only for data rates less than approximately 3 Gbps.

For the analysis of higher-order transfer function a simplified model of transmission path is described in Fig. 3. Multi gigabit serial link design sometimes requires routing a printed circuit board (PCB) signal conductor with two different reference planes. Fig. 3 depicts this situation in which the propagating signal current jumps from signal layer 1 to signal layer 2 through the use of an electrical via. Due to two different reference planes being used on the return path, an impedance discontinuity arises at the location of the electrical via. This impedance discontinuity is due to the capacitance between the power and ground planes that is intended to be part of the return path. At the location of the via, a displacement current component will allow the return current to follow alongside the via until it encounters the power plane, in which the power plane then carries the return current alongside the signal current. In addition to the local capacitive impedance discontinuity occurring from the capacitor that is connected between the power and ground planes at the location of the via, parasitic capacitances also occur between the via and the two reference planes (C_{VIA}). In this model, the impedance discontinuity between the power and ground planes is modeled as a series R-L-C circuit, in which C is the local capacitance (C_{PAR}), the variable L_{PAR} is the parasitic inductance associated with the capacitance, and R_{PAR} is the parasitic resistance of the capacitor.

For a 1000 μm thick PCB with power and ground planes located on the outer surfaces of the PCB, measurements of the local impedance between these two planes yielded values of $C_{PAR} = 400$ pF, $L_{PAR} = 1.2$ nH, and $R_{PAR} = 0.8$ Ω. The parasitic via capacitances C_{VIA} were also determined to be 0.5 pF. For smaller separation distances between the power and ground planes, it is expected that Cp-g would increase in value, while L_{PAR} and R_{PAR} would both decrease in value. The via inductance L_{VIA} was also determined to be 2.4 nH.

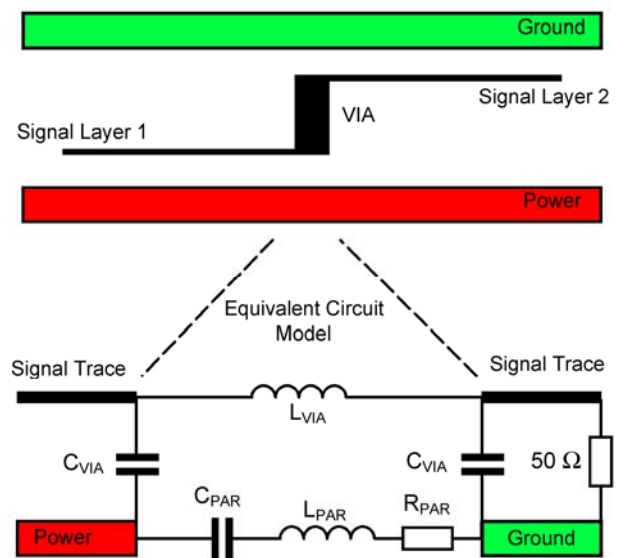


Fig. 3 Equivalent circuit model for transmission channel with higher-order transfer function.

This higher-order transfer function for model described above is shown in Fig. 10. In the first case a transmission line effect is neglected and does not affect the frequency response of the system. It is assumed that the load is matched to the transmission line, so that the only discontinuity that should appear on the frequency response is due to the signal jumping between the power and ground planes. As can be seen from Fig. 10, jumping between power and ground planes causes a bandpass response with only 400pF of capacitance between the power and ground planes. In addition, a strong resonance occurs at about 3GHz. The bandpass result is highly undesirable since it will cause drooping of the flat-top portion of the input signal to appear on the output signal. The resonance is also highly undesirable since it can cause signal ringing.

B. Channel Losses

Losses that need to be considered by the PCB designer can be summarized as conductor and dielectric losses. Conductor losses include DC, skin effect and surface roughness losses. The trade-off associated with foil roughness and conductor loss with the requirement for robust packaging-the challenge is to optimize conductor loss while ensuring good dielectric / foil adhesion [16], [7]. In [13], [18] is shown that the dispersive effects of the dielectric material forming a microstripline can cause reduced transmission bandwidths that are manifested as reduced received pulse amplitudes for the pulses propagating down the line. It is obvious that dispersive effects are almost negligible when conductor heights (h) are less than about 762 μm . The dispersive effects appear to be much more sensitive to changes in h than to changes in conductor widths (W). In addition to these undesirable effects, dispersion can cause reductions in the intended characteristic impedances of the microstripline. Differential transmission line can be designed to match the typically 100 Ω . This reduction in the impedance can be as high as about 5 Ω up to 10 GHz, which corresponds to a rise time of about 50 ps [13]. Other results in [18] show how dispersion affects the effective propagation delays. The higher frequencies will propagate with larger delays than the lower frequencies. The spread in the effective propagation delays can be mitigated by keeping h small, as well as keeping W small. The spreading of the propagation delays is maximized for large h and large W . For example, the spread in propagation delays for $h = 1.524$ mm and $W = 0.381$ mm is about 2 ps/cm between 1 GHz and 10 GHz. More information can be found in [13], [18], [19]. Existing industry-standard insertion loss estimation techniques assume that the copper conductors (PCB traces) are smooth, when in fact they are not. The error thus induced is less significant at lower speeds, but cannot be ignored at frequencies above a few GHz. A known defect of the existing algorithms is that they assume that the copper conductor trace is perfectly smooth. At typical PCB trace dimensions 75-175 μm wide and 15-35 μm thick, and at speeds below 1 GHz, the effect of surface roughness can be neglected. Typically, the "teeth" on the surface of foils that face the interior of the laminate (core material) "sandwich" can be up to 8 μm in depth. The surface roughness of the copper layers will have no effect on current at low frequencies as, at low frequencies, the

depth of current penetration will exceed the value of h . At high frequencies, however (i.e., in the GHz region), the skin effect will be significant. The increase in the conductor loss is governed by (1) [19].

$$\alpha_{cr} = \alpha_c \cdot \left[1 + \frac{2}{\pi} \arctan \left(1.4 \cdot \left(\frac{\Delta}{\delta_s} \right)^2 \right) \right] \quad (1)$$

where α_{cr} is attenuation for rough surface, α_c is attenuation for smooth surface, δ_s is skin depth, Δ is RMS surface roughness.

The following surface plots show the variation of the conductive, dielectric and total losses on the geometry of the coplanar strips at frequency 5 GHz. Differential stripline pair is analyzed in Fig. 4. Total loss estimation is shown in Fig. 5.

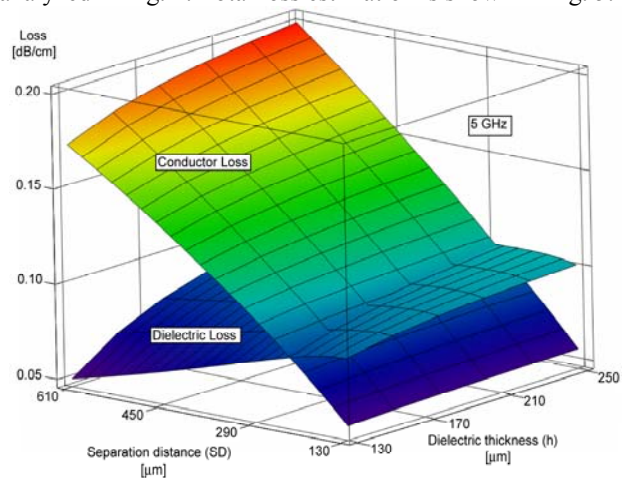


Fig. 4 The variation of the conductive and dielectric losses on the geometry of the coplanar strips at frequency 5 GHz.

It is clearly seen that for analyzed backplane the dielectric losses dominate at higher data rates. The effect of copper roughness is not included in this analysis. Further analysis is focused on determining the total channel losses, and the effect of copper roughness is included.

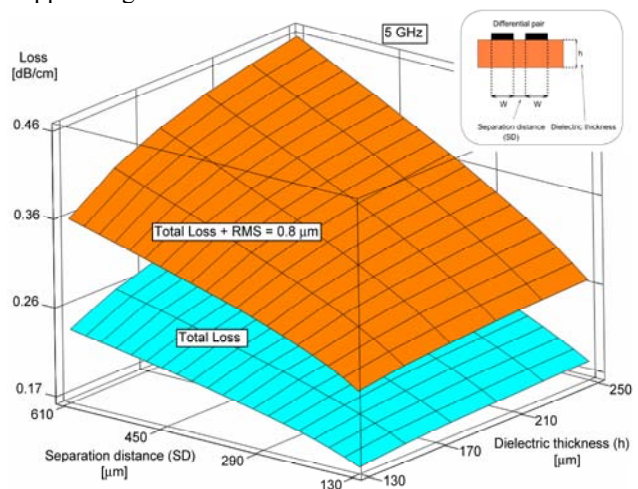


Fig. 5 The variation of total losses on the geometry of the coplanar strips at frequency 5 GHz.

For our analyzed PCB backplane the total losses may increase more than 3 dB due to the roughness effect. Just, this value approximately corresponds to the error achieved between ADS transmission channel model simulation and practical measured results at Nyquist frequency $f_N = 2.5$ GHz for 5 Gbps data rate. As can be seen in previous chapter this channel quality reduction can cause total communication system unreliability. In Fig. 6 the conductor, dielectric and total losses for frequency variation are shown. There are clearly seen the crossover frequencies in which the dielectric losses exceeds the conductive losses. The Fig. 6 highlights these losses for the case in which $W = 130 \mu\text{m}$, $h = 200 \mu\text{m}$, and the edge-to-edge separation distance is $130 \mu\text{m}$. For small edge-to-edge distances of about $130 \mu\text{m}$, the crossover frequency is 2 GHz. For larger separation distances of about $500 \mu\text{m}$, the crossover frequency is much larger.

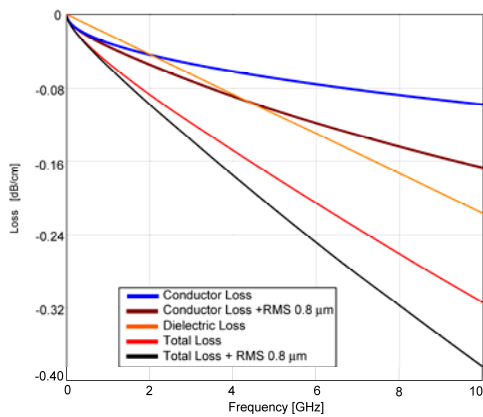


Fig. 6 The variation of conductor, dielectric and total losses versus frequency.

C. Crosstalk Analysis

The analysis describes the differential crosstalk between an aggressor microstripline circuit and a victim differential microstripline circuit, as shown in Fig. 7 and Fig. 8, respectively.

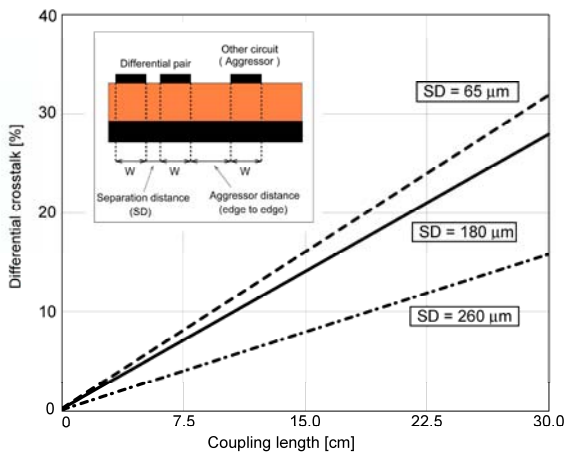


Fig. 7 The variation of differential crosstalk on the geometry of the differential microstrip lines.

It is of interest to predict the impact of tightly or loosely coupled differential conductors on the crosstalk from other circuit. With respect to crosstalk, a differential receiver takes the difference between the crosstalk levels from each of the two differential signal conductors. The main result from the simulations in Fig. 7 is that the differential crosstalk is relatively insensitive to the edge-to-edge spacing between the two differential conductors. It is obvious that the differential crosstalk is linearly dependent on coupling length. Solid lines in both graphs correspond to the proposed PCB backplane structure. The aggressor distance is varied from $65 \mu\text{m}$ to $260 \mu\text{m}$. The significant differential crosstalk reduction (less than 5 %) can be achieved only for aggressor distance greater than $100 \mu\text{m}$ with consider separation distance value $SD = 180 \mu\text{m}$ for designed evaluation backplane.

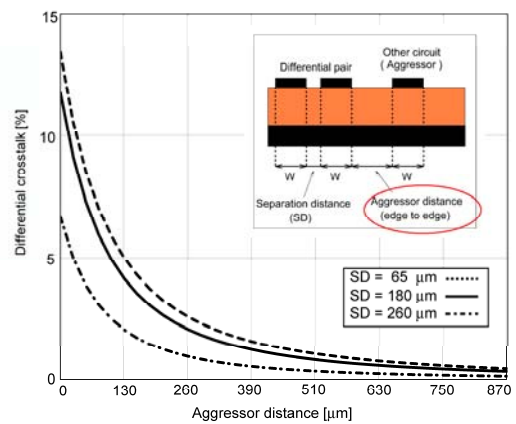


Fig. 8 The variation of differential crosstalk depending on the aggressor distance

Both varied parameters above can be displayed as a surface plot in Fig. 9. These three plots show that for differential microstripline circuits up to 25 cm in length, the separation distance does not have a significant impact on reducing the differential crosstalk or better words the linear dependence is still maintained.

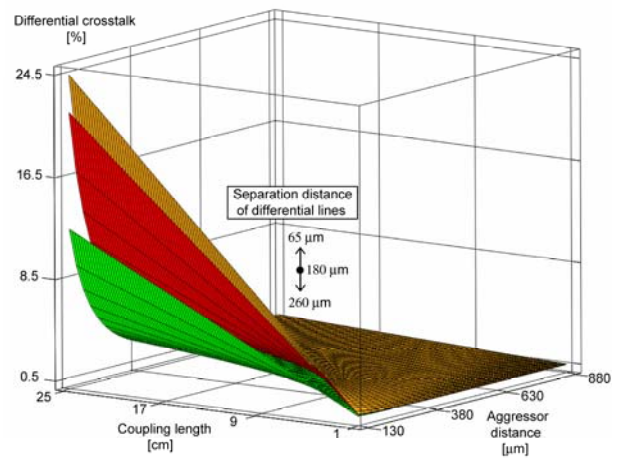


Fig. 9 The variation of differential crosstalk on the geometry of the coplanar strips at frequency 5 GHz.

The simulation results show that the variation in the differential crosstalk is less than 15% for separation distances up to 260 μm . The crosstalk analysis reflects impact of the highest frequencies of the disturbing signal since they tend to couple onto susceptible signals more easily than the lower frequency. The performance of pre-emphasis techniques described in the next chapter is strongly dependent on accurate channel analysis. The evaluation PCB backplane which is originally realized for 5 Gbps data rate signaling is insufficient for data rates higher than 3 Gbps. The realized simulations shows that analyzed channel have 20 dB loss at Nyquist frequency $f_N = 2.5$ GHz (5 Gbps), see [13]. Practical measurement results shows 23 dB loss at the same Nyquist frequency, see Fig. 1.

III. TRANSMITTER PRE-EMPHASIS

Equalization at the transmitter is often called transmitter pre-emphasis to reflect the effect of the filter operation. Various types of equalizers are also commercially available [21], [22]. The main purpose of this filter is to provide a high-pass filtering effect to the signal. In a digital signal, the highest-frequency content is contained in rapid transitions between logic states, while low-frequency content is contained in portions of the signal that do not make transitions.

A. 2-Tap Symbol-Spaced FIR (SSFIR)

Transmitter equalization filter is commonly realized as FIR filters [23], [24], [25]. The purpose of this operation is to increase (decrease for de-emphasis, see below) amplitude for the first bit after a logic transition relative to successive bits. In Fig. 10, the simulated impulse responses of SSFIR filter for two types of the transmission line bandwidth are shown. The standard 2-tap FIR equalized pulse $p_{fir}(t)$ is defined by two coefficients c_1 and c_2 to denote the values of the first and second FIR taps, respectively. A good fit to PCB backplane is obtained by choosing $c_1 > 0$ and $c_2 < 0$, while $|c_1| > |c_2|$. These conditions are applicable similarly for transmitter de-emphasis used in PCI Express. The de-emphasis is comparable alternative which reflects the fact that the equalization is done by reducing the amplitude of the repetitive bits in the light of CMOS processes where actually the maximum voltage swing is pushing below 1.0 V and just PWM pre-emphasis which will be present later can be better solution for these applications. The sum of the absolute values of all tap weights has to be limited to the value of the supply. Therefore the maximum signal swing limit (for both pre-emphasis and de-emphasis, output swing normalized to $\pm 1\text{V}$) places a constraint on the coefficients settings for an equalizer according to [6], [8]

$$\sum_i |c_i| = 1 \quad (2)$$

A theoretical channel (CH1 and CH2) was used to perform the time domain simulations, see Fig. 10. The losses of the channels are monotonously increasing and they are approximately 10 dB at the Nyquist frequency of 2.5 GHz for first BW_{3dB} setting. The second BW_{3dB} setting reflects the

theoretical channel designed to have more pre-cursor ISI where a three-tap filter is usually used and approximately 20 dB loss at the same Nyquist frequency is achieved.

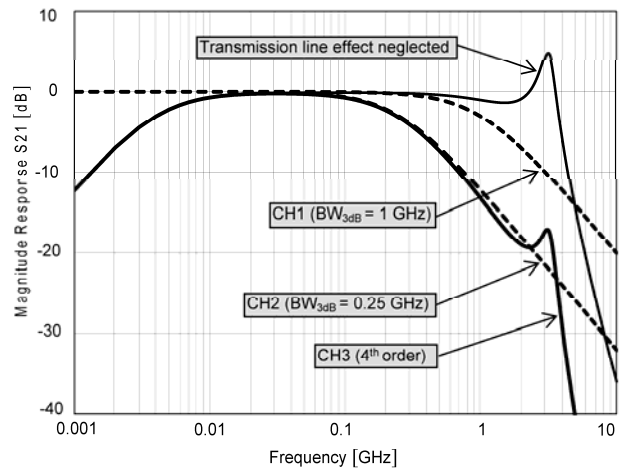


Fig. 10 Two theoretical channel responses for different BW_{3dB} setting and analyzed higher-order transfer function

From the simulated time domain response for two BW_{3dB} setting is clearly seen that optimal pre-emphasis is different for each type of transmission channel. Note that for optimal r parameter settings for each channel the channel output pulse becomes much narrower than the response to a plain NRZ pulse ($r = 1$, $d = 100\%$). This reduces the ISI contributions significantly.

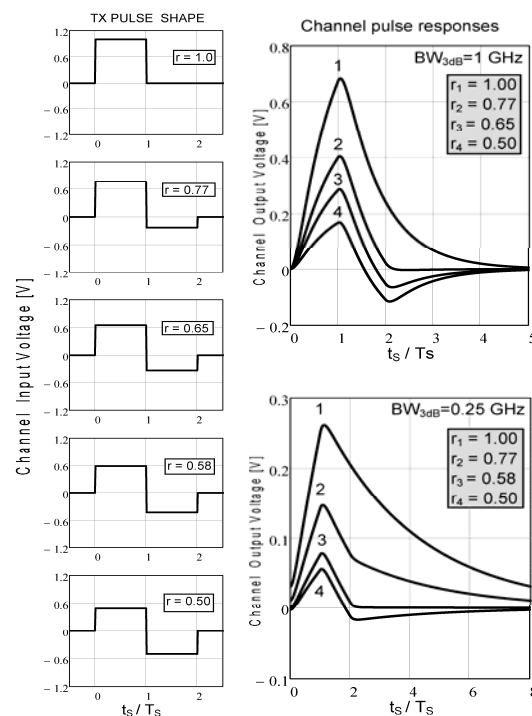


Fig. 11 TX pulse shapes ($T_S = 200$ ps) of SSFIR filter with various r parameter settings and simulated channel pulse responses for two transmission line bandwidth (BW_{3dB}) settings.

The coefficients for time domain simulations are rewritten as $c_1 = r$, $c_2 = r-1$ with $r \in \{0.5...1\}$, resulting in one coefficient r that simply controls the shape of the filter transfer function. Function $p_{fir}(t)$ can be simply formulated as

$$p_{fir}(t) = \begin{cases} 0 & t < 0 \\ r & 0 \leq t < T_s \\ r-1 & T_s \leq t < 2 \cdot T_s \\ 0 & 2 \cdot T_s \leq t \end{cases} \quad (3)$$

where r and $r-1$ denote the values of the first and the second FIR taps, respectively, and T_s represent the symbol duration ($T_s=200$ ps).

B. Pulse-Width Modulation Pre-Emphasis (PWMPE)

In Fig. 12, the simulated impulse responses of PWMPE filter for two type of the transmission line bandwidth are shown. The PWM pulse shape is similar to Manchester code for duty-cycle (d) parameter setting to 50 %. A duty-cycle of 100% corresponds to transmission of normal polar NRZ, compare Fig. 11 and Fig. 13. The optimal duty-cycle setting is strongly dependent on channel characteristics as well as r parameter adjustment at SSFIR pre-emphasis filter. However, it is obvious that the optimal value of both r and d parameters is similar for the same BW_{3dB} setting. Already, this analysis shows that to achieve the same effect for a pulse ISI minimization the SSFIR filter must be used with the stronger pre-emphasis. Note that for the duty-cycle $d = 65$ %, the channel ($BW_{3dB} = 0.25$ GHz) output pulse is in practice as narrow as the FIR pulse where r parameter is set to 0.58. In this case the ISI has been significantly removed. The PWM pulse $p_{pwm}(t)$ is defined as follows, see Fig. 13

$$p_{pwm}(t) = \begin{cases} 0 & t < 0 \\ 1 & 0 \leq t < d \cdot T_s \\ -1 & d \cdot T_s \leq t < T_s \\ 0 & T_s \leq t \end{cases} \quad (4)$$

where d denotes the duty-cycle ($0.5 < d < 1$ fits best to PCB backplane) and T_s again represent the symbol duration ($T_s = 200$ ps).

It can be seen that the PWMPE is capable of narrowing the channel pulse response, similar to FIR pre-emphasis. In practice, PWM duty-cycle d can be adapted to the channel automatically using return channel communication and control algorithm. The need for a return channel is a disadvantage compared to receiver equalization [13], [18] but it is common among all pre-emphasis approaches [24], [25]. In [23], [26], [27] the practical results of PWMPE implementation are shown but only for copper cables. This PWMPE method for copper cables can achieve a loss compensation of 33 dB at 5 Gb/s, which is the highest figure compared to those found in literature [26], [27]. None of the pre-emphasis filters that use 2 taps SSFIR offer more than 18 dB higher loss compensation.

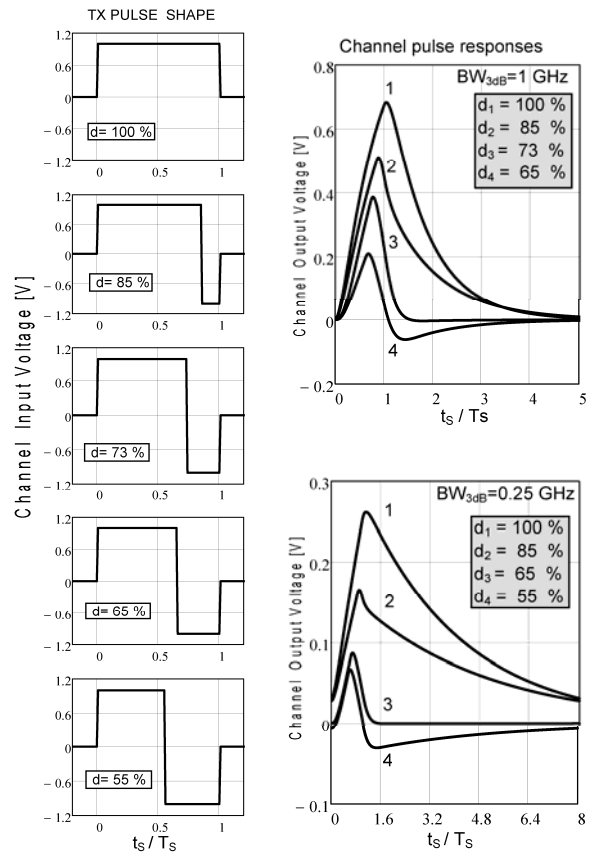


Fig. 12 TX pulse shapes ($T_s= 200$ ps) of PWMPE filter with various duty-cycles settings and simulated channel pulse responses for two transmission line bandwidth (BW_{3dB}) settings.

C. Transfer Function Analysis

Another part of the pre-emphasis methods analysis is focused on calculation of the Power Spectral Density (PSD). To be able to calculate the frequency transfer functions for both filters and compare them the stochastic method for calculation PSD is used. [28]. The SSFIR pulse $p_{fir}(t)$ is defined as in (2) but the pulse is time-shifted according to Fig. 13b. The transmitter (TX) output swing is normalized to $\pm 1V$ as can be seen in Fig. 12. The spectrum $P_{fir}(f)$ of the SSFIR pulse is calculated by taking the Fourier transform of $p_{fir}(t)$ with timing conditions according to Fig. 13b

$$P_{fir}(\omega) = \int_{-\infty}^{+\infty} p_{fir}(t) \cdot e^{-j\omega t} dt = \int_{-T_s}^0 r \cdot e^{-j\omega t} dt + \int_0^{T_s} (r-1) \cdot e^{-j\omega t} dt \quad (5)$$

The PSD_{FIR} by taking (5) and using the formula for PSD of the stochastic signal [28] to account leads to:

$$PSD_{FIR}(\omega) = \frac{|P_{fir}(\omega)|^2}{T_s} \sum_{k=-\infty}^{k=\infty} R(k) \cdot e^{j\omega k T_s} = \frac{\left| \frac{1}{j\omega} \cdot (r \cdot e^{j\omega T_s} + (1-r) \cdot e^{-j\omega T_s} - 1) \right|^2}{T_s} \sum_{k=-\infty}^{k=\infty} R(k) \cdot e^{j\omega k T_s}$$

$$= 2 \cdot \frac{(r^2 - r) \cdot (1 - \cos(2\omega Ts)) - \cos(\omega Ts) + 1}{\omega^2 Ts} \quad (6)$$

where $P_{fir}(\omega)$ is the Fourier transform of $p_{fi}(t)$ and $R(k)$ is the autocorrelation function for a well known polar NRZ signaling and is completely calculated in [28].

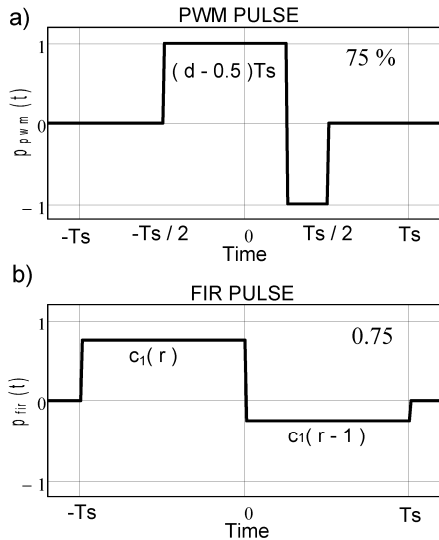


Fig. 13 Definition of pulse shapes for calculating PSD function: a) PWMPE, b) SSFIR.

The function is graphically illustrated for three different r values in Fig. 14. Note that the situation with $r=1$ corresponds to normal polar NRZ line coding. Note how the spectrum is shaped for lower r values when low frequencies are more suppressed then higher frequencies around the Nyquist frequency (0.5 on the x-axis).

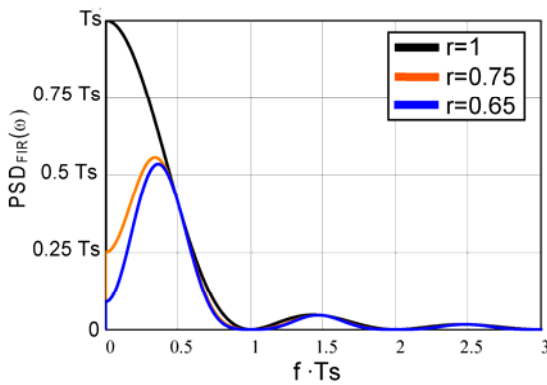


Fig. 14 Power spectral densities for the FIR pulse

Similarly as in the previous case the spectrum of the PWM pulse is calculated by taking the Fourier transform of $p_{pwm}(t)$ with timing condition according to Fig. 13a:

$$P_{pwm}(\omega) = \int_{-\infty}^{+\infty} p_{pwm}(t) \cdot e^{-j\omega t} dt = \int_{-Ts/2}^{(d-0.5)Ts} e^{-j\omega t} dt + \int_{(d-0.5)Ts}^{Ts} -e^{-j\omega t} dt \quad (7)$$

Now let us calculate the power spectral density $PSD_{P_{PWM}}$ for the PWM filter as

$$PSD_{P_{PWM}}(\omega) = \frac{|P_{pwm}(\omega)|^2}{T_s} \sum_{k=-\infty}^{k=\infty} R(k) \cdot e^{j\omega k T_s} = 2 \cdot \frac{3 - 2\cos(\omega(d-1)Ts) - 2\cos(\omega d Ts) + \cos(\omega Ts)}{\omega^2 Ts} \quad (8)$$

where $P_{pw}(\omega)$ is the Fourier transform of $p_{pw}(t)$ and $R(k)$ is the autocorrelation function for a well known polar NRZ signaling (because $R(k)$ is the same for PWM as for polar NRZ) and is completely calculated in [24].

This function is shown in Fig. 15. It is obvious that the spectrum is shaped and moved to higher frequencies. The spectrum is more boosted at higher frequencies above Nyquist frequency (0.5 on the axis) approximately for d values from 0.65 or less. It can be important factor for higher performance to compensate more lossy channels. Now for both presented pre-emphasis can be calculated the frequency domain transfer functions. It is important to know how filter transfer function is capable to fit better channel response for high-speed signaling. This function is illustrated in Fig. 16 for SSFIR filter. The several values for r were chosen to show the range of possible equalizer gains. It is obvious that for the closer r value ($r = 0.5$), more low-frequency attenuation the filter exhibits.

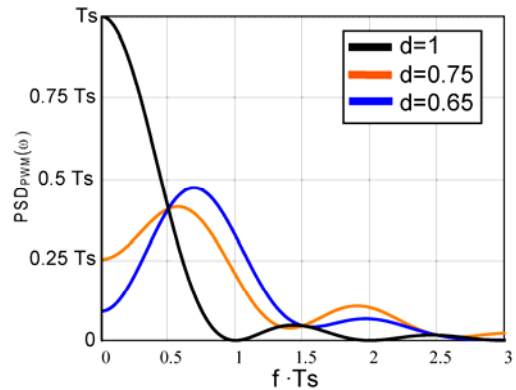


Fig. 15 Power spectral densities for the PWM pulse.

The frequency transfer function response for FIR filter can be calculated as follows:

$$H_{FIR}(\omega) = \frac{P_{fir}(\omega)}{P_{NRZ}(\omega)}, \quad (9)$$

where $P_{fi}(\omega)$ is the Fourier transform of $p_{fi}(t)$ and P_{NRZ} is the spectrum of normal polar NRZ pulse with defined width T_s and height 1 which is known as

$$P_{NRZ}(f) = \frac{2}{\omega} \cdot \sin(\omega T_s / 2). \quad (10)$$

The expression for $H_{FIR}(\omega)$ with taking the modulus yields into account is defined as

$$|H_{FIR}(\omega)| = \sqrt{1 + (r^2 - r) \cdot \frac{\cos(2\omega T_s) - 1}{\cos(\omega T_s) - 1}} \quad (11)$$

The expression for $H_{PWM}(\omega)$ with taking the modulus yields into account is defined as

$$|H_{PWM}(\omega)| = \sqrt{2 \frac{\cos(\omega(d-1)T_s) + \cos(\omega d T_s) - 2}{\cos(\omega T_s) - 1} - 1} \quad (12)$$

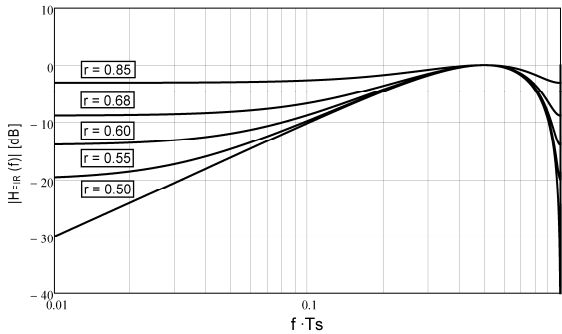


Fig. 16 Calculated magnitude of FIR filter transfer function. Note that f_N is at 0.5 on the x-axis.

Comparing the PWMPE and SSFIR transfer functions in Fig. 16 and Fig. 17 respectively, it can be seen that for low frequencies both filter exhibit the same behavior. However in the high frequency (HF) range, at frequencies just below f_N , the PWM filter behaves differently. Due to the time-varying behavior of the PWM filter, near $2f_N$ the effective gain of the PWM filter increases to infinity. The PWM filter transfer function can be seen as a higher order filter with only one parameter [26].

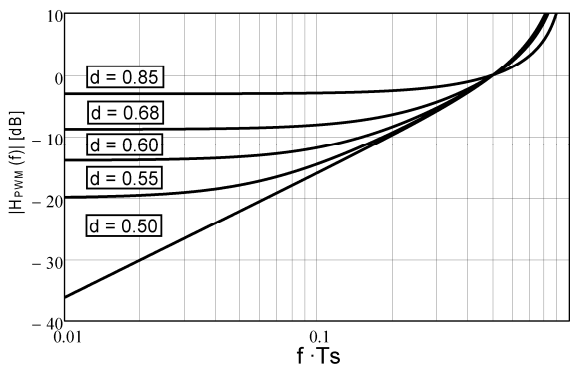


Fig. 17 Calculated magnitude of PWM filter transfer function. Note that f_N is at 0.5 on the x-axis.

While both filters have a different slope at f_N , their transfer at f_N is equal: both filters leave the amplitude of the fastest data transitions ('101010') unchanged. This is precisely what a pre-emphasis filter for these channels should do. Ideally, the equalizer should attenuate all frequencies below f_N and leave the fastest transitions untouched [6]. This is valid for the channel where attenuation increases monotonically with frequency, as is shown in Fig. 10. Practical measurement

show that at frequencies just above 1 GHz the channel losses are comparable with theoretical channel ($BW_{3dB} = 0.25$ GHz).

D. Equalized channel transfer function

Two theoretical channels described above are used to calculate the equalized channel transfer function for the SSFIR filter and the PWMPE filter, see Fig. 10. The results for SSFIR filter and PWMPE filter are shown in Fig. 18 and Fig. 19 respectively. The first theoretical channels ($BW_{3dB} = 1$ GHz) is analyzed.

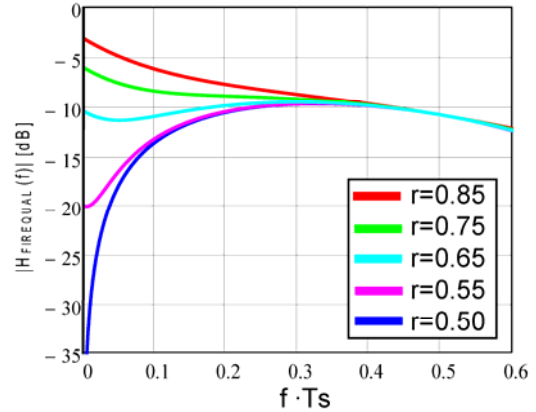


Fig. 18 Equalized channel transfer function of first theoretical channel ($BW_{3dB} = 1$ GHz). SSFIR filter is used.

The equalized transfer function is calculated by taking the two theoretical channel responses and multiplying it with calculated theoretical transfer functions of the pre-emphasis filters. A bit length $T_s = 200$ ps corresponds with bit period for 5 Gbps data rate. The values for r parameter and d parameter are chosen around the optimal values which can be analyzed for each channel, see Fig. 11 and Fig. 12. Now the flatness in the frequency interval $[0, f_N]$ is analyzed. Again, note that f_N is at 0.5 on the x-axis. The channel response for SSFIR pre-emphasis is flat more than 5dB, see Fig. 18, while the PWMPE response is flat less than within 3 dB, see Fig. 19 for optimal channel r and d parameter setting.

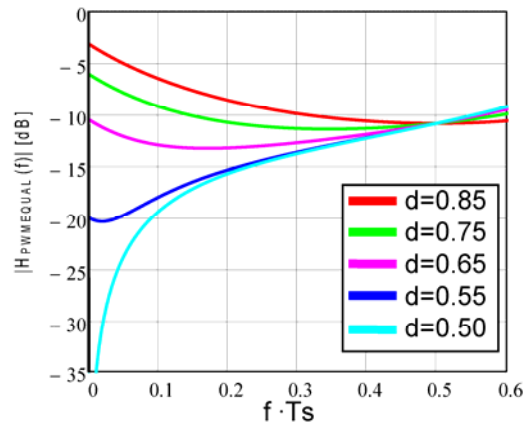


Fig. 19 Equalized channel transfer function of first theoretical channel ($BW_{3dB} = 1$ GHz). PWMPE filter is used.

The situation for second theoretical channel with higher losses ($BW_{3dB} = 0.25$ GHz) is somewhat different. It is obvious that for optimal r parameter setting $r = 0.58$ in the case of SSFIR filter the curve flatness is still increasing to approximately 8 dB, see Fig. 20. The equalized channel by PWMPE filter has still similar flatness as in the previous case for optimal d parameter setting $d = 0.65$ (65%), see Fig. 21. For shorter PCB backplane lengths the responses become flatter because the smaller losses must be compensated. For PCB backplane with higher losses the increasing curve flatness indicates insufficient compensation leading to complete eye closure for high-speed signaling.

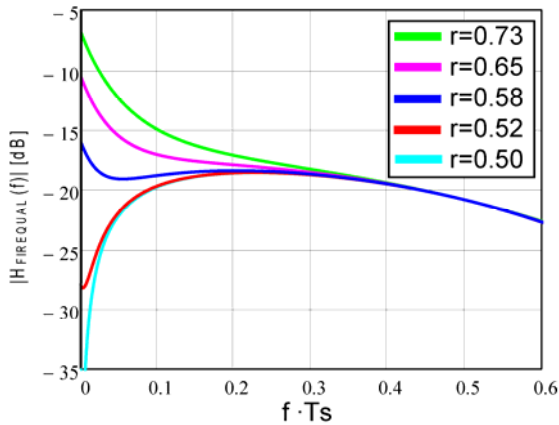


Fig. 20 Equalized channel transfer function of first theoretical channel ($BW_{3dB} = 0.25$ GHz). SSFIR filter is used.

This situation can be seen in the previous equalized channel transfer functions where e.g. for less lossy channel the strong pre-emphasis can cause more curve flatness in the frequency interval $[0, f_N]$. Conversely, for more lossy channel the still increasing curve flatness for the closer r or d value indicates the pre-emphasis insufficiency to overcome the increasing channel losses.

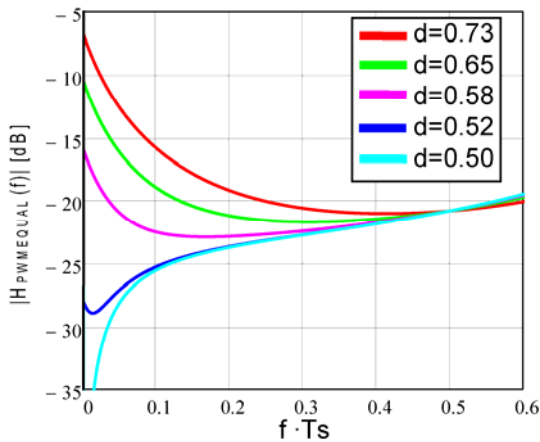


Fig. 21 Equalized channel transfer function of first theoretical channel ($BW_{3dB} = 0.25$ GHz). PWMPE filter is used.

Similarly, the equalized transfer function of channel with higher-order transfer function was performed. The decisive factor for the performance of the proposed equalizer is how the overall swing is reduced in order to achieve the reduction in minimum-to-maximum loss for the system. This “flattening” of the magnitude of the frequency response described above is a good qualitative way to view the benefit of equalization. In the first case the SSFIR filter is analyzed, see Fig. 22. The reduction in the loss variation (note that our maximum loss is at Nyquist frequency 2.5 GHz) in our example approximately triples the frequency at which the eye closes completely from 0.5 to 1.5 GHz.

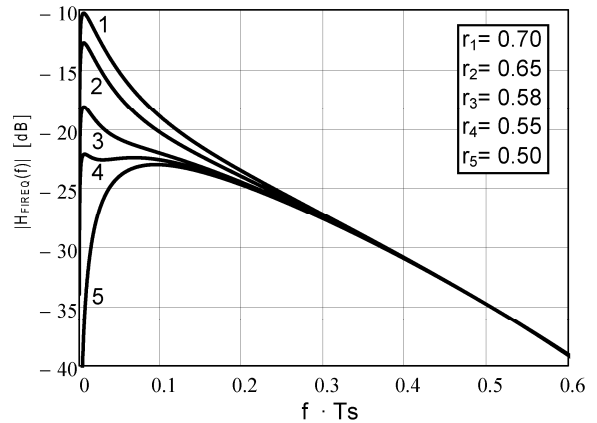


Fig. 22 Equalized channel with high-order transfer function (CH3). SSFIR filter is used.

In the case of PWMPE filter the total variation in the loss decreased from -6 dB to -20 dB for the maximum (strong) pre-emphasis effect ($d = 0.50$), see Fig. 23. The reduction in the loss variation in our example allows to shift the frequency at which the eye closes completely from 0.5 to 2.5 GHz. It is obviously that this reduction will allow us to extract more performance from the system by running at a substantially higher data rate up to 5 Gbps.

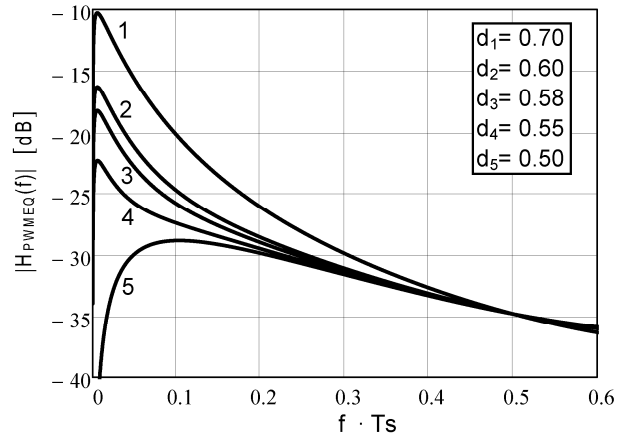


Fig. 23 Equalized channel with high-order transfer function (CH3). PWMPE filter is used.

E. Eye Diagram performance

The effect of adjusting the d parameter of the PWMPE filter and r parameter of the SSFIR filter can be seen in Fig. 24 and Fig. 25, respectively. The left and right edges in the eye diagrams correspond to the symbol edges. It can be seen that the best eye response is for optimum d parameter and r parameter setting ($BW_{3dB} = 1\text{GHz}$), see Fig. 11 and Fig. 12. Both under-emphasis and over-emphasis are also shown.

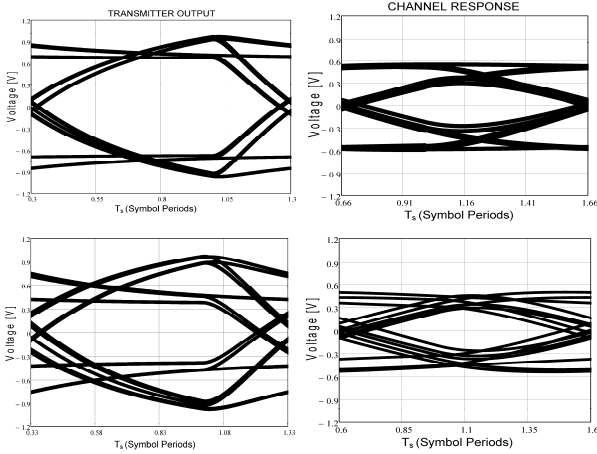


Fig. 24 Simulated transmitter eyes and channel response for transmitter settings at 5 Gb/s; first case: optimal pre-emphasis (75 %), second case: strong pre-emphasis (60 %).

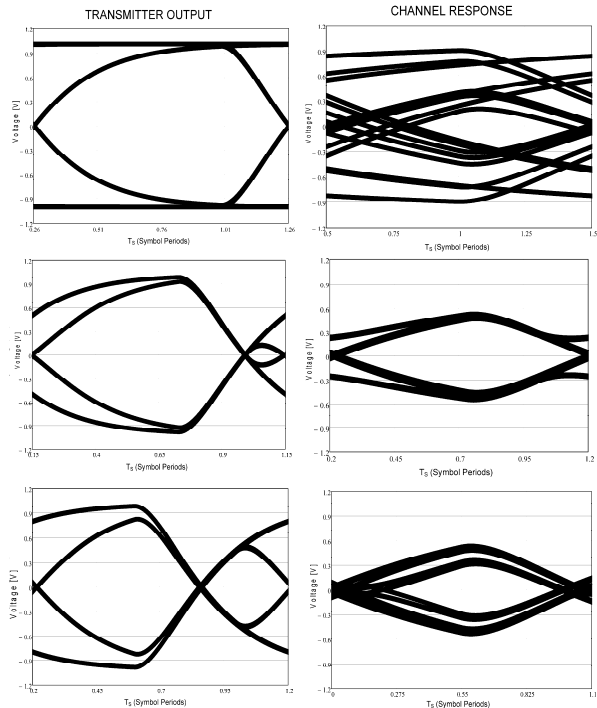


Fig. 25 Simulated transmitter eyes and channel response for transmitter settings at 5 Gb/s; first case: no pre-emphasis (100 %), second case: optimal pre-emphasis (73 %), third case: strong pre-emphasis (60 %). Horizontal axis = 50 ps/div, vertical axis = 300 mV/div.

Note that the time scale is the same for all eyes. The pre-emphasis leaves the fastest pattern unchanged while it attenuates the slower transitions. Note the better eye opening for PWM bit stream than for FIR pulses at the same conditions. The eye height is approximately the same for both filters up to ~ 20 dB PCB loss at $f_N = 2.5$ GHz. After that, the eye of the 2-tap SSFIR is completely closed and PWMPE still has an open eye, up to ~ 26 dB.

The optimum value of pre-emphasis is the crossover point between the two plots, as it provides a trade-off between the value of eye height and eye width (blue line), see Fig. 26 for PWMPE and Fig. 27 for SSFIR. The optimum PWMPE level for transmission channel with 25 dB loss at Nyquist frequency $f_N = 2.5$ GHz is thus found to be around $d = 55\%$.

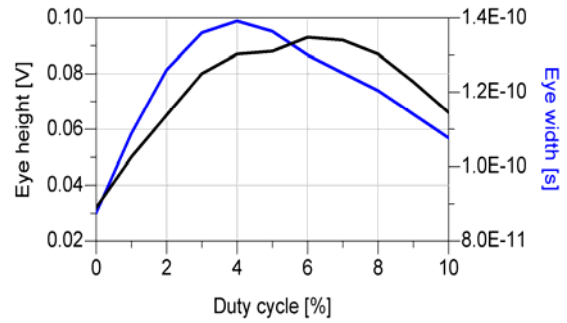


Fig. 26 Determination of the optimal PWMPE level for transmission channel with 25 dB loss at Nyquist frequency $f_N = 2.5$ GHz.

The SSFIR filter is insufficient for channel with 25 dB loss at the same Nyquist frequency. Details for this analysis can be found in [13]. Note that value on x-axis is multiplied by 10.

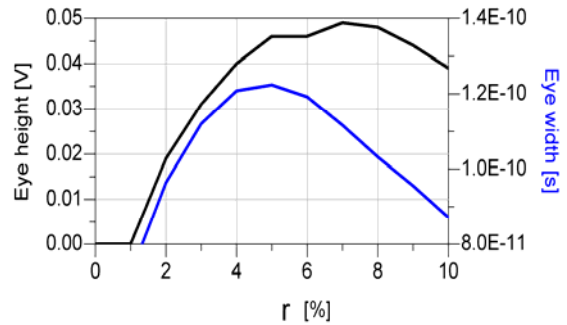


Fig. 27 Determination of the optimal PWMPE level for transmission channel with 25 dB loss at Nyquist frequency $f_N = 2.5$ GHz.

IV. MEASURED RESULTS

To evaluate the performance of both pre-emphasis techniques the backplane prototype was created. Two types of backplanes are compared. The First backplane represents the channel with small losses and without impedance discontinuities comparable with channel response CH1 in Fig. 10. The second channel represents the more lossy channel comparable to CH2 in Fig. 10 with failure in the ground layer and closely-spaced transmission lines (cross-talk effect). The measured output eyes for both channel is shown in Fig. 28.

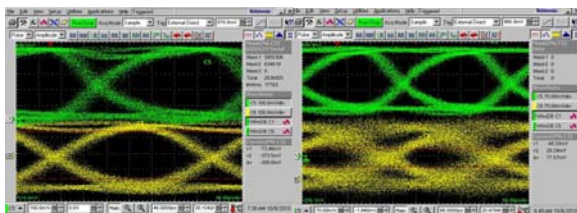


Fig. 28 Measured eyes of channel responses at 3.125 Gb/s for two type of transmission channels; left: transmitter .output and channel output (channel without failure); .right: transmitter output and channel output (channel .with failure).

In Fig. 29 measured output eyes for two values of pre-emphasis is shown. Inadvertent value of pre-emphasis may cause further eye closing and the channel output response can be degraded more than channel response with pre-emphasis disabled. The maximum data rate is 3.125 Gbps.

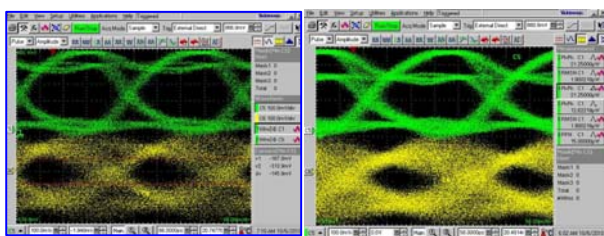


Fig. 29 Measured eyes of channel responses of transmission channel (channel with failure) at 3.125 Gb/s; left: transmitter output for optimal pre-emphasis SSFIR (67%) setting and channel output, right: transmitter output for strong pre-emphasis SSFIR (57%) setting and channel output.

V. CONCLUSIONS

A new digital pre-emphasis technique based on pulse-width modulation (PWM) is introduced. In the first part of the paper, advanced modeling of channel losses is described in brief. It is obvious that channel losses can be predicted with sufficient accuracy. The PWM method does not tune the pulse amplitude (as for FIR pre-emphasis), but instead exploits timing resolution. This fits well for today and the future low voltage high-speed CMOS processes. Using a theoretical channel with differential transmission line, successful transmission of a 2-PAM 5 Gbps data signal over the channel with 25 dB is demonstrated. From advanced theoretical analysis it can be concluded that the pre-emphasis is capable to compensate enough channel loss to enable error free transmission at 5 Gbps. The available data rate for practical results is 3.125 Gbps. It corresponds to a 14 dB loss compensation at the fundamental frequency $f_N = 1.56$ GHz. The highest figure compared to literature on 2-tap FIR pre-emphasis filters is about 18 dB loss. The PWM pre-emphasis filter can be adjusted to the PCB backplane using only a single coefficient (the duty cycle). A 5-tap FIR filter in [10] reaches 30 dB but only at 3.125 Gbps. More taps can offer higher loss compensation but their cost of increasing complexity, possibly causing accuracy and speed issues.

For more complex channel transfer function the better results with PWM pre-emphasis are achieved. It is obvious that PWM pre-emphasis is able to equalized channel of 4th order transfer function with 20 dB loss at Nyquist frequency 2.5 GHz. Other results show that the FIR pre-emphasis method is more suitable to compensate the channel with 1st order transfer function. For more complex channel transfer function it is necessary to use FIR filter with more taps. The mathematical modeling of transmission lines via numerical methods for the solution of hyperbolic partial differential equations, based on finite differences can be found in [29]. Further research will focus on more detailed analysis of PWMPE filter in practical measurement.

REFERENCES

- [1] P. Jirava and J. Krupka, "Classification model based on rough and fuzzy sets theory", *Proceedings of the 6th WSEAS International Conference on Computational Intelligence, Man-Machine Systems and Cybernetics*, pp. 198-202, 2007.
- [2] M. Doumpos and A. Salappa, "Feature selection algorithms in classification problems: an experimental evaluation", *WSEAS Transactions on Information Science & Applications*, vol. 2, no. 2, pp. 77-82, 2005.
- [3] G. Fuchs, A. Staindl, and S. Jakubek, "Order Reduction for a Realtime Engine Model Using Flat and Nonlinear Galerkin Methods". *In Proceedings of International Conference Advances in Communications, Computers, Systems, Circuits and Devices ECS'10*, Puerto De La Cruz, Tenerife, Canary Islands (Spain), 2010, pp. 255-260. ISBN: 978-960-474-250-9.
- [4] M. Kamiński, Symbolic Computations in Science and Engineering, *In Proceedings of 12th WSEAS International Conference on COMPUTERS*, Heraklion, Greece, July 23-25, 2008, pp. 10251031
- [5] B. Ahmad, J. Cain, "Performance evaluation of high speed serial links," *DesignCon 2001*.
- [6] S.H. Hall, H. Heck, *Advanced Signal integrity for High-Speed Digital Design*, John Wiley & Sons. New Jersey, 2009.
- [7] Adam, J.; Chi Shih Chang; Stankus, J.J.; Iyer, M.K.; Chen, W.T., "Addressing packaging challenges," *IEEE Circuits and Devices Magazine*, vol. 18, Issue 4, July 2002, Pages: 40 - 49.
- [8] H. Johnson, M. Graham, *High-Speed Digital Design: A Handbook of Black Magic*, Prentice Hall 1993.
- [9] J. Howard, M. Graham, *High-Speed Signal Propagation: Advanced Black Magic*, Prentice Hall, 2003.
- [10] R. Farjad-Rad, C.-K. Yang, M. Horowitz, T. Lee, "A 0.3- μ m CMOS 8-Gb/s 4-PAM Serial Link Transceiver," *IEEE Journal of Solid-State Circuits*, vol. 35, no. 5, May 2000, pp. 757-764.
- [11] H. Partovi *et al*, "A 62.5 Gb/s multi-standard SerDes IC," *IEEE Custom Integrated Circuits Conference*, Sept. 2003, pp. 585-588.
- [12] C.-K. Yang, R. Farjad- Rad, M. Horowitz, "A 0.5- μ m CMOS 4.0-Gbit/s serial link transceiver with data recovery using over sample *Circuits*, vol. 33, no. 5, May. 1998, pp. 713-722.
- [13] B. Ševčík. and L. Brančík, "Signal Integrity Problems in the Design of High-Speed Serial Communication Device". *In 33rd International Conference on Telecommunications and signal processing TSP - 2010*, Baden near Vienna, Austria, 2010, pp. 426-431. ISBN: 978-963-88981-0-4.
- [14] Agilent Technologies. Advanced Design System ADS2009, Evaluation version [Online]. Available: <http://www.home.agilent.com>.
- [15] MathCAD, Inc. (2005). Mathcad Evaluation Version 13 [Online]. Available: <http://www.mathcad.com>.
- [16] V. Stojanović, M. Horowitz, "Modeling and Analysis of High-Speed Links," *IEEE Custom Integrated Circuits Conference*, September 2003.
- [17] J. Zerbe, C. Werner, R. Kollipara, V. Stojanovic, "A Flexible Serial Link for 5-10Gb/s in Realistic Backplane Environments," *DesignCon 2004*.

- [18] B. Sevcik, L. Brancik. "Analysis and Modeling of Signal Integrity Problems in the Serial Communication Devices". In *Mathematical Models for Engineering Science (MMES 10)*. Puerto De La Cruz, Tenerife, Canary Islands, Spain: 2010. s. 172-178. ISBN: 978-960-474-252-3.
- [19] R. Kollipara, G-J Yeh, B. Chia, A. Agarwal, "Design, Modeling and Characterization of High-Speed Backplane Interconnects," *DesignCon 2003*.
- [20] S. Wu *et al.*, "Design of a 6.25-Gbps Backplane SerDes with Top-Down Design Methodology," *DesignCon 2004*.
- [21] V. Stojanovic, Channel- limited high-speed links: modeling, analysis and design , Ph.D. Dissertation, Stanford University, September 2004.
- [22] B. Ševčík. "High- Speed Serial Differential Signaling Links with Commercial Equalizer." In *Proceedings of 20th International Conference Radioelektronika 2010*, 2010, Brno, pp. 191-194. ISBN: 978-1-4244-6319-0.
- [23] H. Cheng and A. C. Carusone, "A 32/16 Gb/s 4/2-PAM transmitter with PWM pre-emphasis and 1.2 Vpp per side output swing in 0.13 μm CMOS," in *Proc. 2008 Custom Integr. Circuits Conf. (CICC)*, 2008, pp. 635–638.
- [24] W. Gai, Y. Hidaka, Y. Koyanagi, J.H. Jiang, H. Osone and T. Horie, "A 4-channel 3.125 Gb/s/ch CMOS transceiver with 30dB equalization", *Symposium on VLSI Circuits, Digest of Technical Papers*, pp. 138-141, 2004.
- [25] W.J. Dally and J. Poulton, "Transmitter equalization for 4 Gb/s signaling," *IEEE Micro*, vol. 17, no. 1, pp. 48-56, Jan.-Feb. 1997.
- [26] J.-R. Schrader, E. A. M. Klumperink, J. L. Visschers, and B. Nauta, "Pulse-width modulation pre-emphasis applied in a wireline transmitter, achieving 33 dB loss compensation at 5-Gb/s in 0.13- μm CMOS," *IEEE J. Solid-State Circuits*, vol. 41, no. 4, pp. 990–999, Apr. 2006.
- [27] J. Schrader, E. Klumperink, and B. Nauta, "Wireline equalization using pulse-width modulation," in *Proc. 2006 Custom Integr. Circuits Conf. (CICC)*, 2006, pp. 591–598.
- [28] L.W. Couch, *Digital and analog communication systems*, Prentice-Hall, 2001.
- [29] L. Brančík and B. Ševčík, " Modeling of Nonuniform Multiconductor Transmission Lines via Wendroff Method." In *Proceedings of the International Conference on Mathematical Models for Engineering Science (MMES 10)*. Puerto De La Cruz, Tenerife, Canary Islands, Spain: 2010. s. 130-133. ISBN: 978-960-474-252-3.

B. Sevcik was born in Prostejov, Czech Republic, in 1985. He received his MSc. degree in 2009 from the University of Technology, Brno. He is currently studying his Ph.D. study at the same university. His research interest is in analysis and design of analog circuits, high-speed transmission lines design and signal integrity computer optimization methods. He is author and coauthor of several papers in international conference proceedings.

L. Brancik was born in Kyjov, Czech Republic, in 1961. He received his MSc. degree in 1985 from the Brno University of Technology, candidate of technical sciences (CSc.) in 1993 from the Brno University of Technology, in 2000 he was promoted to Docent. He is currently professor of theoretical electrical engineering at the Brno University of Technology. His research interest is in numerical methods for electronics circuits, computer optimization methods and signal integrity analysis. He is author and coauthor of several papers in international journals and conference proceedings.

M. Kubiček was born in Svitavy, Czech Republic, in 1983. He received his M.Sc. from the Brno University of Technology in 2001. Since then, he has been pursuing his Ph.D. degree at the Department of Radio Electronics at the same university. He is concerned with FPGA-based digital systems. His work is focused on high speed data transmissions, data processing and embedded systems.